New Journal of Physics
The open-access journal for physics

Double-resonance lineshapes in a cell with wall coating and buffer gas

Svenja Knappe[1] **and Hugh G Robinson**
NIST, Time and Frequency Division, Boulder, CO 80305, USA
E-mail: knappe@boulder.nist.gov

New Journal of Physics **12** (2010) 065021 (9pp)
Received 30 November 2009
Published 28 June 2010
Online at http://www.njp.org/
doi:10.1088/1367-2630/12/6/065021

Abstract. Microwave double resonances were measured in a wall-coated Rb vapor cell as a function of additional buffer-gas pressure. These data were compared with similar measurements in an uncoated cell. It was found that the linewidth in the coated spherical cell of diameter 1.6 cm displays a distinct maximum around 0.2 kPa. This agrees well with theoretical solutions of the diffusion equation, assuming a complex reflection coefficient at the wall. It was also found that at intermediate pressures the lineshapes of the microwave resonances become asymmetric with a low-frequency tail. This agrees with the explanation that where the alkali mean free path is substantially smaller than the average distance between wall collisions at zero pressure, there exist two classes of atoms in the cell. The atoms that get trapped near the walls accumulate much larger phase shifts than those toward the center of the cell. This effect is not seen in the longitudinal relaxation rate, indicating that it is related to a phase-shift effect.

Contents

1. Motivation **2**
2. Theoretical calculations **2**
3. Experimental setup **4**
4. Experimental results **5**
4.1. Experimental lineshapes 5
4.2. Resonance linewidth as a function of nitrogen pressure 7
5. Conclusions **9**
References **9**

[1] Author to whom any correspondence should be addressed.

© IOP Publishing Ltd and Deutsche Physikalische Gesellschaft

1. Motivation

For many decades, two methods have been known to reduce resonance broadening of ground-state transitions in alkali vapor cells due to collisions of the atoms with the container walls. The first method is to add to the vapor cell so-called buffer gases, inert or diatomic gases with low polarizability that have little effect on the ground states of the alkali atoms. This method is routinely used in commercial vapor cell devices such as atomic clocks and magnetometers. The second method is nearly as old as the first and uses anti-relaxation wall coatings [1]. These coatings usually consist of paraffin waxes or silanes with long carbohydrate chains. If the container walls are coated with such substances, the atom can survive up to 10 000 collisions before the ground-state polarization is destroyed [2]. Buffer gases have been studied extensively and they are used often because of their ease of use and predictable behavior, but the use of wall coatings can have some distinct advantages. Buffer gases pressure-broaden the excited states of the alkali atoms. This can limit the hyperfine pumping efficiency once the broadening exceeds the ground-state hyperfine splitting frequency ($\sim$ 3–10 GHz) and therefore degrade the performance of atomic vapor cell clocks. For devices that rely on alignment in atoms, such as coherent population trapping (CPT) clocks with linearly polarized light [3, 4], frequency-modulated nonlinear magneto-optical rotation (FMNMOR) [5, 6] or double resonance alignment magnetometers (DRAM) [7], the restrictions are even tighter; the pressure broadening should not exceed the excited state hyperfine splitting (less than 1.2 GHz), because of destructive interference in the excited states. Detailed discussions of CPT and FMNMOR signals with partially resolved hyperfine structures can be found in [8] and [9], respectively. This problem can become aggravated when very small vapor cells are used [10]. In these cases, the use of wall coatings could be advantageous.

For magnetometers, wall coatings are attractive, because the sensitivity to magnetic field gradients is much reduced as compared to that for buffer-gas cells [11]–[13]. This is because every atom still samples the entire cell, which results in an effect known as 'motional narrowing'. Finally, optical rotation signals can be much larger in wall-coated cells as compared to buffer-gas-filled ones, since the signal size becomes proportional to the lifetime of the excited state at higher pressures [14, 15].

One question that can arise, of course, is whether the simultaneous use of a buffer gas and a wall coating can be advantageous for certain applications. This regime has not been studied in great detail. In this paper we compare the effects of random motion of rubidium atoms in a cell with and without wall coating and with a buffer gas at pressure p on the hyperfine frequency and linewidth. The mathematics of such motion has been treated in the case of neutron transport [16, 17]. For alkali atoms, this regime has been studied for hyperfine transitions [18] (also described in [19]) and on Zeeman transitions for longitudinal relaxation [20] and transverse relaxation [21].

2. Theoretical calculations

In order to calculate the relaxation of the atoms in the presence of a wall coating and a buffer gas, we follow the approaches of Masnou-Seeuws and Bouchiat [22], who used it to calculate T_1, and Wu *et al* [21], whose approach for nuclear spins includes both T_1 and T_2. We assume that the evolution of the atomic polarization $P(\vec{r}, t)$ can be described by the diffusion equation,

$$\frac{\partial P(\vec{r}, t)}{\partial t} = D\nabla^2 P(\vec{r}, t) - \gamma_{\mathrm{p}} P(\vec{r}, t), \tag{1}$$

where $D = D_0 p_0/p$ is the diffusion constant, normalized to normal pressure p_0 The spin-destruction rate $\gamma_p = v_{rel}\ \sigma_p p/k_B T$ depends on the depolarization cross-section σ_p and the relative velocity v_{rel} between alkali and buffer-gas atoms. Both, D and γ_p, depend on the buffer-gas pressure, p. As boundary conditions, we assume a spherical cell with radius r_0, and contrary to many approaches, we do not force the polarization to be zero at the walls. Following the approach of [21, 22], we write the polarization current towards the wall at the position of the wall as

$$j_+ = n_{Rb} v_{Rb} \left[\frac{P}{4} - \frac{\lambda_{MFP}}{6} \frac{\partial P}{\partial n} \right]_{r=r_0}, \tag{2}$$

with the Rb density n_{Rb}, thermal velocity v_{Rb} and mean-free path $\lambda_{MFP}= 3D/v_{Rb}$. The vector $\vec{n}$ is orthogonal to the wall. The reflected current,

$$j_- = R \cdot j_+ = R_0 e^{-i\delta} \cdot j_+, \tag{3}$$

includes the complex reflection coefficient R with amplitude R_0 and phase-shift per collision δ [21]. The solution for the fundamental diffusion mode is

$$P(\vec{r}, t) = \frac{\sin(kr)}{kr} e^{-\Gamma t}, \tag{4}$$

where k is the spatial frequency, and

$$\Gamma = \gamma_D + \gamma_p \tag{5}$$

is the relaxation rate due to wall and diffusion effects ($\gamma_D = Dk^2$) and buffer-gas depolarization (γ_p).

To simplify the equations, we define two additional parameters, A_0 and Θ, related to the reflection coefficient,

$$A_0\, e^{-i\Theta} \equiv \frac{1-R}{1+R}. \tag{6}$$

When equations (1) and (4) are combined, we can derive the boundary condition equation,

$$\tan(kr_0) = \frac{kr_0}{1-\zeta^{i\Theta}}, \tag{7}$$

with $\zeta = A_0\, v_{rel}\, r_0/2D$. Equation (7) can be solved numerically. We can then deduce the decay rates $\Gamma = C_s\ (kr_0)^2/3\zeta$, with $C_s = 3A_0\, v_{rel}/2r_0$. At zero pressure, the contribution of the coating reduces to $\gamma_D(p = 0) = C_s e^{i\Theta}$.

The full linewidth and shift of the resonance due to collisions with the wall are then given by the real and imaginary parts of the relaxation rate, respectively,

$$\Delta\nu_{width} = \mathrm{Re}[\Gamma]/\pi \tag{8}$$

and

$$\delta\nu_{shift} = \mathrm{Im}[\Gamma]/2\pi\,. \tag{9}$$

For the case $p = 0$, we can then define the number of collisions before transverse depolarization N_2 as the ratio between the lifetime T_2 and average time between wall collisions τ_c (for a spherical cell $\tau_c = 4r_0/(3v_{Rb})$),

$$N_2 = \frac{T_2}{\tau_c} = \frac{A_{02}}{2} \cos\Theta. \tag{10}$$

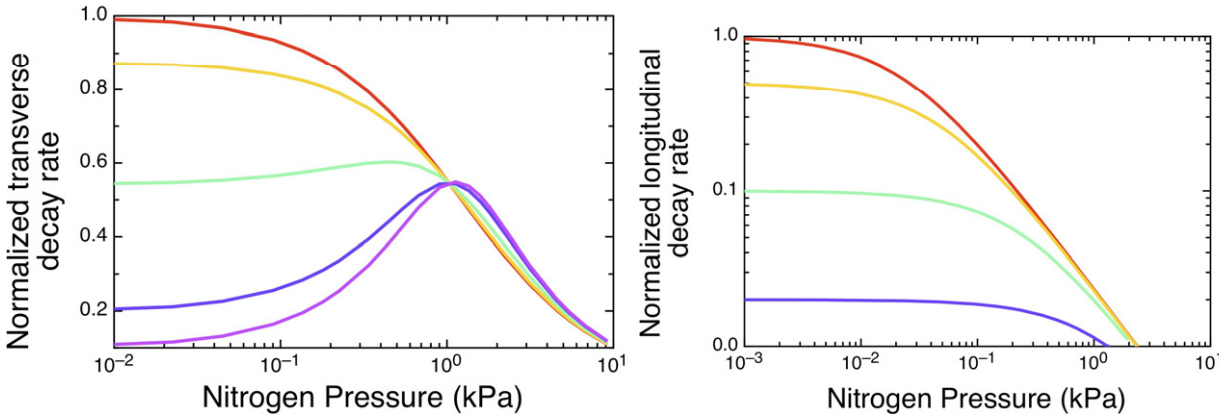

Figure 1. (Left) Transverse relaxation rate (T_2) normalized to rate at $p = 0$ as a function of nitrogen pressure and different phase shifts (red: $\Theta = 0$, orange: $\Theta = 0.5$, green: $\Theta = 1$, blue: $\Theta = 1.37$, purple: $\Theta = 1.47$). (Right) Normalized longitudinal relaxation rate (T_1) as a function of nitrogen pressure for different wall qualities (red: $A_{01} = 1$, orange: $A_{01} = 0.5$, green: $A_{01} = 0.1$, blue: $A_{01} = 0.02$). All other parameters remained the same as in (a).

In an equivalent way, the number of collisions before longitudinal relaxation can be defined for T_1 relaxation. Despite the fact that we do not measure the longitudinal relaxation rates experimentally, we present the theory here because it can give more insight into the different relaxation mechanisms of T_1 and T_2. Since in the case of T_1 no phase shifts are induced during the collisions, a real reflection coefficient R can be used, i.e. $\delta = 0$ (and therefore $\Theta = 0$) and

$$N_1 = \frac{T_1}{\tau_c} = \frac{A_{01}}{2}. \tag{11}$$

In figure 1(a), the microwave transverse relaxation rate is plotted as a function of buffer-gas pressure for different values of Θ. It is normalized to the relaxation rate of a cell with no coating ($R = 0$). It can be seen that as $\Theta \to \pi/2$, the coating becomes better, i.e. the resonance linewidth at low pressures narrows. At very high pressures, decoherence is dominated by buffer-gas collisions and therefore the linewidth is independent of the coating. The direct decoherence effects due to collisions of alkali and buffer-gas atoms, i.e. γ_p, were neglected in this graph. When included, the linewidth starts to increase again at higher buffer-gas pressures, similar to the behavior seen in pure buffer-gas cells. In the intermediate region, the linewidth is very sensitive to the behavior of the coating; at some intermediate pressures, the linewidth actually increases as the coating becomes better. At first sight, this is very counter-intuitive. It is an effect that is seen in T_2 relaxation only. For the longitudinal relaxation T_1, $\Theta = 0$, and the decay rate does not show a local maximum, as can be seen in figure 1(b); the longitudinal decay rate is depicted for different wall qualities. A similar behavior was seen by Boulanger [18] and it was suggested that this can be explained by two classes of atoms: those that get trapped near the walls and accumulate a large phase shift, and those toward the center of the cell.

3. Experimental setup

Hyperfine double resonances were measured for the same ^{87}Rb vapor cell with anti-relaxation wall coating at various buffer-gas pressures. In order to vary the pressure inside the cell

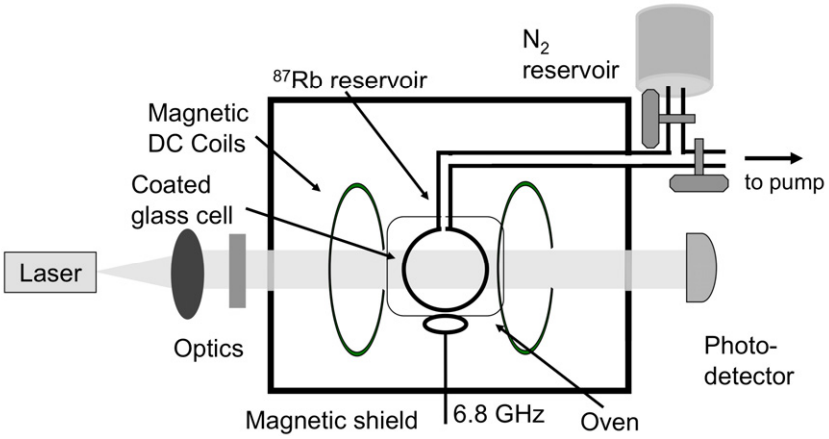

Figure 2. Schematic of the experimental setup.

without removing it from the system, it was connected to a buffer-gas reservoir through a metal valve. A capacitance manometer was used to determine the buffer-gas pressure inside the cell. A schematic of the experimental setup is shown in figure 2. The glass cell has a diameter of 1.6 cm. It is coated with tetracontane, an n-alkane with chemical formula $C_{40}H_{82}$. It was connected to the cell stem through an orifice of roughly 1 mm diameter. The stem served as the Rb reservoir and also had a connection to a glass-to-metal seal that allowed access to a vacuum system. The system included a buffer-gas reservoir, a pressure gauge and a turbo pump. It enabled changes in the buffer-gas type and pressure inside the cell. The vapor cell was held inside a copper oven with bifilar resistive heaters and was mounted inside a mu-metal shield. The currents that drove the bifilar resistive heaters were switched on and off at a frequency of 7.5 Hz. A dc magnetic field of a few microtesla to lift the degeneracy of the Zeeman levels was produced by the set of coils collinear with the laser beam.

The light from a vertical-cavity surface-emitting laser at 795 nm was linearly polarized and directed through the Rb cell. The transmitted light was detected on a photodetector. The light was resonant with the $|5S_{1/2}, F = 2\rangle \leftrightarrow |5P_{1/2}, F' = 1\rangle$ transition, to optically pump the atoms into one of the ground-state hyperfine states. A radiofrequency (RF) field with a frequency of about 6.8 GHz was applied to the cell through a small loop antenna, located close to the bottom of the cell. The frequency of the RF field was scanned around the transition frequency of the two hyperfine $m_F = 0$ Zeeman sublevels, while the transmitted laser intensity was recorded. The photodiode signal is fed into a lock-in amplifier that was gated such that the signal was measured only while the heating currents were off, in order not to influence the resonance by possible heating magnetic fields.

4. Experimental results

4.1. Experimental lineshapes

Double-resonance spectra of the 0–0 microwave transition were recorded for a variety of nitrogen buffer-gas pressures between 0 and 25 kPa. The shifts of the resonance frequency gave an indication of the buffer-gas pressure, independent of the pressure gauge. These shifts could not be used as a precise measurement because the resonance frequency also depends on

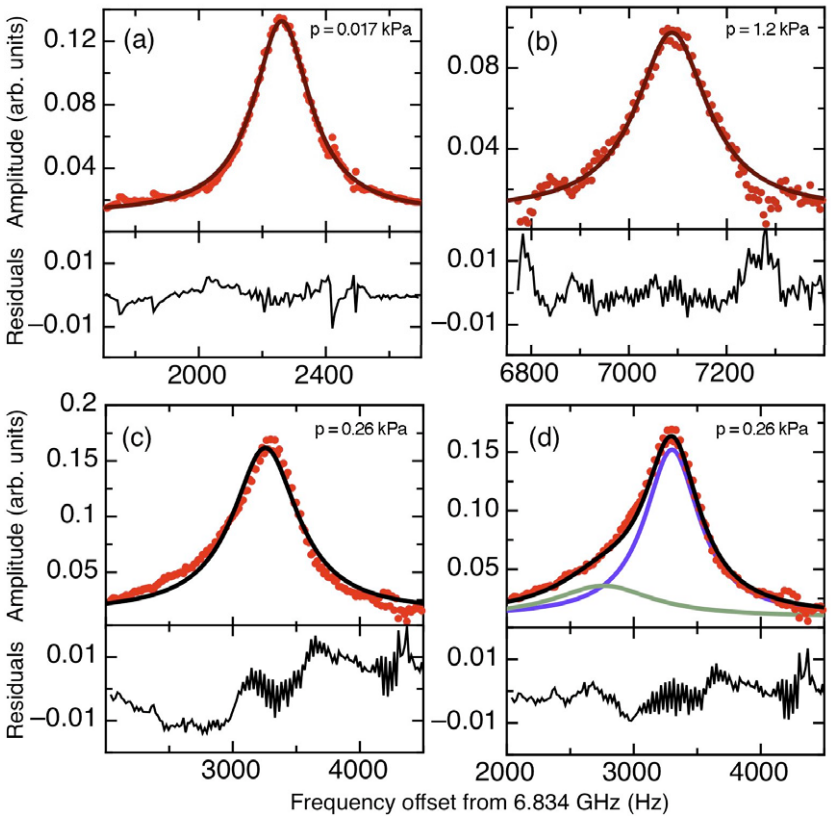

Figure 3. Microwave resonance spectra measured for nitrogen pressures of 0.017, 0.26 and 1.2 kPa, respectively. Solid lines in (a)–(c) are single Lorentzian fits to the data. The black solid line in (d) is a fit of two Lorentzians added together. The two individual Lorentzians are shown as green and blue solid lines as well. The residuals are shown below.

the wall interactions that were to be studied here. Therefore, it could not be assumed that the shift due to the wall remained constant for all pressures. First, the cell was evacuated and the buffer-gas pressure was increased slowly. The nitrogen pressure was then lowered again until the cell was finally evacuated. The resonances at zero pressure were compared before and after these measurements, and it was found that the wall coating was not significantly altered by the addition of nitrogen. The spectra were measured at very low optical and microwave power to ensure that the resonance lines were not significantly power broadened. The temperature of the cell was kept at about 22 °C.

The spectra were fitted with Lorentzian lineshapes. Figure 3 shows spectra at three different pressures: 0.017, 0.26 and 1.2 kPa. The red dots are the measured values, while the black solid lines are the Lorentzian fits. It can be seen that the fits match the measurements well at low and high pressures, but at intermediate pressures between 0.1 and 0.5 kPa a low-frequency tail seems to be present. This behavior was repeatable for different coatings, cell sizes and beam positions.

The microwave field is applied to the cell with a loop antenna near the cell, which causes an inhomogeneous field distribution. In order to rule out the possibility that the line asymmetry was caused by magnetic microwave field gradients, spectra were measured at two different beam

diameters, ∼1 and ∼5 mm. The lineshapes show no significant difference in the asymmetry for both beam diameters. At least at higher pressures, where the atoms are more localized, inhomogeneities in the microwave field should cause asymmetries that depend on the location of the beam.

This seems to indicate that microwave field gradients are not causing this asymmetry. Whereas in cells without buffer gas and at very low pressures the lineshapes are expected to be symmetric, because all atoms average over the whole cell volume, at high pressures the atoms are confined to smaller regions of the cell. The fact that the spectra are symmetric at higher pressures is another indication that microwave field gradients are not causing the observed asymmetry. We furthermore investigated lineshapes for a cell without wall coating for a variety of pressures, and we found them always to be symmetric, adding to the conclusion that the asymmetry in coated cells with intermediate buffer-gas pressures is not caused by microwave field gradients.

The region where the asymmetry occurs roughly coincides with the region of the local maximum in the linewidth (see figure 1(a)). An explanation for this behavior is that above some intermediate pressures the cell becomes divided into two regions [18, 19]; some atoms become trapped near the wall and undergo wall collisions at a higher rate, accumulating a large phase shift. They should therefore show a broader resonance line with larger negative frequency shift than for atoms at the center of the cell. The fact that this asymmetry is not seen at higher pressures could be explained as being because the depolarization distance decreases with buffer-gas pressure. Therefore, the number of atoms interacting mainly with the wall decreases with an increase in linewidth. Due to the fraction of atoms trapped in the center of the cell by the buffer gas, the signal increases. This causes the observed increase in the narrower symmetric component. This explanation is also in agreement with the fact that the wider component is always found on the low-frequency side; the wall coating shifts the atomic resonance to smaller values. As a crude approach, the asymmetric spectra were fitted with two Lorentzians with two different center frequencies, widths and amplitudes. As can be seen from figure 3(d), this seems to fit the data better, compared with the single Lorentzian. The two components are also shown separately.

4.2. Resonance linewidth as a function of nitrogen pressure

The linewidths extracted from the fits to the spectra are displayed in figure 4 as a function of nitrogen pressure. For intermediate pressures, two Lorentzians are fitted to the spectra, and the width of the narrower one at higher frequency is plotted. The width in the case without buffer gas was measured before and after exposing the cell to nitrogen and seems to coincide for both measurements. This suggests that the cell was not contaminated during the exposure to buffer gas. The width of the resonance for the evacuated cell indicates a lifetime of $T_2 = 2.4$ ms, which translates to roughly 65 wall collisions before decoherence. For the uncoated cell, all lineshapes are fitted sufficiently with single Lorentzians. The blue fit to the data assumes diffusion and buffer-gas relaxation only. At pressures below an experimentally determined value p_{br}, a turnover was added empirically to the lowest-order diffusion mode solution (see, for example, [23]): $\Gamma = \gamma_{\mathrm{D}}/(p + p_{\mathrm{br}}) + \gamma_{\mathrm{p}} + \gamma_{\mathrm{s}}$. The rate γ_{s} is independent of the buffer-gas pressure and includes the spin-exchange and power-broadening contributions.

The data in figure 4 clearly show the increase in linewidth predicted in section 2. This is not an artifact due to the fitting procedure, since a similar behavior is found if in the intermediate pressure region the data are fitted with a single or a double Lorentzian. The maximum of the

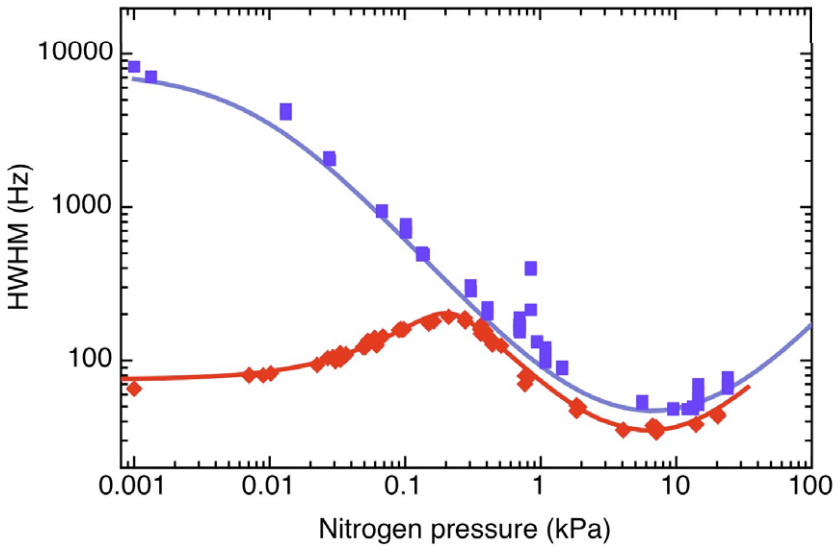

Figure 4. Linewidths of the microwave resonances measured as a function of nitrogen pressure for the paraffin-coated cell (red diamonds) and a bare glass cell (blue squares). The solid lines are fits to the data.

linewidth is found at roughly 0.2 kPa of nitrogen pressure. At this pressure, the mean free path is estimated as $\lambda_{\mathrm{MFP}} = 3D/v_{\mathrm{Rb}} = 0.01$ cm. When taking into account the number of collisions before decoherence, this would result in an effective depolarization length of 0.8 cm, half the diameter of the cell.

For the uncoated cell, the expected linewidth was calculated by taking into account the first-order diffusion mode only and by use of the parameters from [24] for the diffusion constant and buffer-gas relaxation. An offset was fitted to the data to include spin-exchange collisions, the orifice and residual power broadening.

For the data of the coated cell, the theory of section 2 was used to fit the data (see the solid red line in figure 4). Here, the same values were assumed for diffusion and buffer-gas collisions, as for the uncoated cell. Apart from the coating parameters A_{02} and Θ, a scaling factor for the pressure, an amplitude and a constant offset were used in the fits. At $p = 0$ the fit yields a phase shift per collision of $\delta = -0.040(5)$ rad, which is similar to those published previously [25].

Ideally, we should be able to reproduce the data in figure 4 by calculating the properties of the coating from the measurements at $p = 0$ alone, because amplitude and phase shift per collision should be enough to characterize the coating. Nevertheless, we cannot rule out completely that the properties of the coating change slightly in the presence of buffer gas. Furthermore, the simplified theory developed here has several shortcomings that could account for the incorrect scaling; it assumes averaging over the whole cell volume, but already at intermediate pressures the atoms do not sample the whole cell. It might therefore not be sufficient to calculate the results by taking the lowest-order diffusion mode, although this seems to be enough for the longitudinal relaxation [20], but higher-order diffusion modes might have to be taken into account.

5. Conclusions

Good qualitative agreement was found between the measurements of the double-resonance linewidth in a cell with a combination of wall coating and buffer gas and a simple theoretical model. The introduction of an imaginary reflection coefficient predicts a maximum in the transverse relaxation rate that was found in the experimental data. The longer low-frequency tail in the measured spectra is in agreement with the explanation that the maximum is caused by two regions of the cell where atoms get trapped near the walls. Furthermore, the 0–0 microwave linewidths measured in the paraffin-coated cell were compared to those from an uncoated cell. It can be seen that a slight improvement in linewidth can be found by adding the wall coating, but that the improvement decreases rapidly with increased buffer-gas pressure.

This is a contribution of NIST, an agency of the US government, and not subject to copyright.

References

[1] Robinson H, Ensberg E and Dehmelt H 1958 *Bull. Am. Phys. Soc.* **3** 9
[2] Bouchiat M A and Brossel J 1966 *Phys. Rev.* **147** 41–54
[3] Kazakov G, Matisov B, Mazets I, Mileti G and Delporte J 2005 *Phys. Rev.* A **72** 063408
[4] Taichenachev a V, Yudin V I, Velichansky V L, Kargapoltsev S V, Wynands R, Kitching J and Hollberg L 2004 *JETP Lett.* **80** 236–40
[5] Gilles H, Hamel J and Cheron B 2001 *Rev. Sci. Instrum.* **72** 2253–60
[6] Budker D, Kimball D F, Yashchuk V V and Zolotorev M 2002 *Phys. Rev.* A **65** 055403
[7] Domenico G D, Bison G, Groeger S, Knowles P, Pazgalev A S, Rebetez M, Saudan H and Weis A 2006 *Phys. Rev.* A **74** 063415
[8] Wynands R and Nagel A 1999 *Appl. Phys.* B **68** 1–25
[9] Auzinsh M, Budker D and Rochester M D 2009 *Phys. Rev.* A **80** 053604
[10] Kitching J, Knappe S and Hollberg L 2002 *Appl. Phys. Lett.* **81** 553–5
[11] Cates G D, Schaefer S R and Happer W 1988 *Phys. Rev.* A **37** 2877–85
[12] Pustelny S, Jackson Kimball D F, Rochester S M, Yashchuk V V and Budker D 2006 *Phys. Rev.* A **74** 063406
[13] Watanabe S F and Robinson H G 1977 *J. Phys. B: At. Mol. Phys.* **10** 931–9, 941–57, 959–65 and 1167–74
[14] Seltzer S 2008 Developments in alkali–metal atomic magnetometry *PhD Thesis* Princeton University
[15] Seltzer S and Romalis M 2009 arXiv:0906.3054v1
[16] Davison B 1957 *Neutron Transport Theory* (Oxford: Clarendon)
[17] Glasstone S and Edlund M C 1952 *The Elements of Nuclear Reactor Theory* (New York: D Van Nostrand)
[18] Boulanger J S 1975 *PhD Thesis* Universite de Laval
[19] Vanier J and Audoin C 1989 *The Quantum Physics of Atomic Frequency Standards* (Bristol: Adam Hilger)
[20] Seltzer S, Rampulla D M, Rivillon-Amy S, Chabal Y J, Bernasek S L and Romalis M V 2008 *J. Appl. Phys.* **104** 103116
[21] Wu Z, Schaefer S, Cates G D and Happer W 1988 *Phys. Rev.* A **37** 1161
[22] Masnou-Seeuws F and Bouchiat M A 1967 *J. Physique* **28** 406
[23] Beverini N, Minguzzi P and Strumia F 1971 *Phys. Rev.* A **4** 550–5
[24] Vanier J, Simard J F and Boulanger J S 1974 *Phys. Rev.* A **9** 1031–40
[25] Budker D, Hollberg L, Kimball D F, Kitching J, Pustelny S and Yashchuk V V 2005 *Phys. Rev.* A **71** 012903